2011

Interactions of a Mn atom with halogen atoms and stability of its half-filled 3d-shell

Kalpataru Pradhan
Virginia Commonwealth University, kpradhan@vcu.edu

Gennady L. Gutsev
Florida A&M University, gennady.gutsev@famu.edu

Charles A. Weatherford
Florida A&M University

Purusottam Jena
Virginia Commonwealth University, pjena@vcu.edu

Pradhan, K., Gutsev, G. L., & Weatherford, C. A., et al. Interactions of a Mn atom with halogen atoms and stability of its half-filled 3d-shell. The Journal of Chemical Physics, 134, 234311 (2011).

Interactions of a Mn atom with halogen atoms and stability of its half-filled 3*d*-shell

Kalpataru Pradhan,[1] Gennady L. Gutsev,[2] Charles A. Weatherford,[2] and Purusottam Jena[1,a)]
[1]*Physics Department, Virginia Commonwealth University, Richmond, Virginia 23284, USA*
[2]*Department of Physics, Florida A&M University, Tallahassee, Florida 32307, USA*

(Received 18 April 2011; accepted 31 May 2011; published online 21 June 2011)

Using density functional theory with hybrid exchange-correlation potential, we have calculated the geometrical and electronic structure, relative stability, and electron affinities of MnX_n compounds ($n = 1$–6) formed by a Mn atom and halogen atoms X = F, Cl, and Br. Our objective is to examine the extent to which the Mn–*X* interactions are similar and to elucidate if/how the half-filled 3*d*-shell of a Mn atom participates in chemical bonding as the number of halogen atoms increases. While the highest oxidation number of the Mn atom in fluorides is considered to be +4, the maximum number of halogen atoms that can be chemically attached in the MnX_n^- anions is 6 for X = F, 5 for X = Cl, and 4 for X = Br. The $MnCl_n$ and $MnBr_n$ neutrals are superhalogens for $n \geq 3$, while the superhalogen behavior of MnF_n begins with $n = 4$. These results are explained to be due to the way different halogen atoms interact with the 3*d* electrons of Mn atom. © *2011 American Institute of Physics*. [doi:10.1063/1.3601753]

I. INTRODUCTION

Bartlett and Lohmann,[1,2] who found that PtF_6 is capable of oxidizing both an O_2 molecule and a Xe atom whose first ionization potentials are 12.22 eV and 12.17 eV, respectively, impressively demonstrated the high oxidative power of transition metal halides nearly half a century ago. This power is due to a very high electron affinity (EA) of the platinum hexafluoride, which was estimated to be 6.8 eV. The experimental findings helped to outline a class of species named as superhalogens.[3] A typical superhalogen MX_{k+1} is composed of a central metal atom M and halogen atoms X, and *k* is the maximal formal valence of the central atom. It was found that such MX_{k+1} compounds possess[4–6] the electron affinities that are larger than the EAs of the halogen atoms (F: 3.399 ± 0.003 eV; Cl: 3.617 ± 0.003 eV; Br: 3.365 ± 0.003 eV).[7] The earlier work was mainly concentrated on *sp*-superhalogens, such as MX_2 (M = Li, Na; X = Cl, Br, I),[8] MX_3 (M = Be, Mg, Ca; X = Cl, Br),[9–11] MX_4 (M = B, Al; X = F, Cl, Br),[12,13] and MX_6 (M = 3*d*-5*d* metal atoms).[14,15] These studies have been extended to the superhalogens containing transition metal atoms[16–18] as well as to the superhalogens containing oxygen[19–21] and hydrogen[22] as ligand atoms. Currently, there is a surge of interest in the superhalogens and their anions, because the anions play an important role in chemistry as oxidizing agents,[23] nucleation center,[24] biocatalysts, and building blocks of new energetic materials.[25,26]

No exception was found to the superhalogen formula, if the central atom is an *sp*-element. However, it is not straightforward to apply the superhalogen MX_{k+1} concept to transition metal halides, because transition metal atoms exhibit multiple oxidation states. In particular, the oxidation state of Mn atom can vary from 0 [e.g., in $Mn_2(CO)_{10}$] to +7 [e.g., in MnO_4^-] or even be negative. Since the valence electronic configuration of the Mn atom is $3d^5 4s^2$, the maximal formal valence of Mn is to be +7. If this is the case, MnO_4 has to be a superhalogen because the sum of oxygen valencies is one more than 7. Indeed, MnO_4 was found to possess the electron affinity of ~5 eV in combined theoretical and experimental study.[27] However, "the maximal formal valence" of Mn in halides is not clear because its highest oxidation state is +7 in oxides but +4 in fluorides.[28] Therefore, it is interesting to study how the electron affinity of manganese halides depends on the number and type of halogen atoms.

The purpose of the present work is to perform a systematic study on the neutral and singly negatively charged manganese halides MnX_n (X = F, Cl, Br) for all *n* values for which at least one species in a pair MnX_n–MnX_n^- is thermodynamically stable. The preferred oxidation state found for Mn is +2, which is indicative of the participation in the bonding of only 4*s* electrons. One could compare the properties of Mn trihalides with the properties of *sp*-halides whose central atom possesses an ns^2 valence shell as only chemically active. For this purpose, we choose MgX_3 halides because Mg has the valence electronic shell $3s^2$. We use density functional theory with a hybrid exchange-correlation functional in our calculations of the equilibrium geometries, electronic structure, and preferred spin multiplicities of neutral and anionic states. In Sec. II we provide a brief description of our theoretical procedure. In Sec. III we describe the structure and spectroscopic properties of MnX_n and MnX_n^-, and Sec. IV provides a brief summary of the work.

II. COMPUTATIONAL DETAILS

Our computations are performed using the combination of Becke's hybrid 3-parameter exchange functional and

a)Electronic mail: pjena@vcu.edu.

correlation functional of Lee–Yang–Parr referred to as B3LYP.[29] We use a spin-unrestricted version of the B3LYP method. This generally produces spin-contaminated states.[30] It is quite common that spin contamination is large in low-spin states, but is negligible for high-spin states. Since all our Mn halides studied possess high-spin ground states (GS), the spin contamination is rather small and does not exceed 5%. The atomic orbitals are represented by Gaussian 6–311+G(3*df*) basis sets.[31,32] The choice of a proper method is critical in obtaining reliable results,[33–36] and can be based on comparison of the results obtained using a particular method to experiment or on performance of the method for compounds closely related to those under study. As for the experimental data, the photoelectron spectra have been measured for $MnCl_3^-$ and $MnBr_3^-$.[17] Our B3LYP/6-311+G(3*df*) value of 5.05 eV for the vertical detachment energy (VDE) of an extra electron from $MnCl_3^-$ is in fair agreement with the experimental values of 5.6 ± 0.2 eV (Ref. 37) and 5.50 ± 0.06 eV.[17] Our B3LYP VDE value obtained for $MnBr_3^-$ is 4.95 eV, which is also in fair agreement with the experimental value of 5.36 ± 0.06 eV.[17]

Comparison of dozens of different methods was performed using, as the reference, the results obtained by coupled-cluster method with singles and doubles and noniterative triples [CCSD(T)] (Ref. 38) for hexafluorides of 4*d* and 5*d* transition metals.[39,40] It was found that the B3LYP provides the values which are quite close to the corresponding CCSD(T) values, and the B3LYP performance is better than the performance of pure DFT methods in the case of *nd*-metal halides.

Further support to the reliability of the B3LYP/6-311+G(3*df*) level is provided in Table I, where the results of our B3LYP calculations are compared to those of RCCSD(T) calculations performed earlier for MnF.[41] As is seen, the B3LYP values of the bond length and dissociation energy are in excellent agreement with experiment[42,43] and the RCCSD(T) values obtained using a 5-zeta basis set. The B3LYP values, obtained for MnF^+ and MnF^- are also close to the values obtained using the RCCSD(T) approach.

The geometries are first optimized without any symmetry constraint using GAUSSIAN 03 code.[44] Various guess structures with halogen atoms bound to the metal atom both molecularly and chemically were used to determine the ground-state geometries. All possible spin multiplicities are probed in order to determine the total ground-state spin. The convergence threshold for total energies was set to 0.000001 eV and for the forces to 0.001 eV/Å. The lowest energy state geometries were re-optimized within actual symmetry constraints, if such obtained, in order to assign spectroscopic states.

The vibrational frequencies of all cluster states discussed below are positive, which means that their geometries belong to the minima on the potential energy surfaces. Adiabatic electron affinities (EA_{ad}) are calculated as the differences between total energies of the anion and its neutral parent computed at the corresponding ground-state geometries. The VDEs are computed as the differences in total energies of an anion and its neutral parent at the anion ground-state geometry.

III. RESULTS and DISCUSSION

We first discuss the structure of neutral and singly negatively charged Mn chlorides because there are experimental mass spectrometry data, followed by a discussion of our results on neutral and anionic series of Mn bromides and fluorides. Finally, we outline the structure and properties of Mg trihalides since Mg has the same oxidation state as Mn in its most thermodynamically stable halides.

A. $MnCl_n$ clusters

The mass spectra of the $MnCl_n^-$ anions produced in a pulsed arc cluster ion source exhibit rather unusual features.[37] Since Mn oxidation states of +2 and +7 are quite common (e.g., in $MnCl_2$, MnO, and MnO_4^-), one could anticipate that the prominent peaks should correspond to $MnCl_3^-$ and $MnCl_8^-$. However, only a $MnCl_3^-$ peak was observed in the spectra, which shows that the preferable interactions of Cl with Mn are likely divalent. In order to explore the character of Mn–Cl interactions, we optimized the lowest total energy state geometries of $MnCl_n$ and $MnCl_n^-$ shown in Fig. 1 as a function of the Cl amount. The extra electron attachment is accompanied by significant geometry changes, namely, $MnCl_2$ is linear, while $MnCl_2^-$ is bent, the $MnCl_3$ and $MnCl_4$ geometries possess C_{2v} and D_2 symmetry, respectively, while the $MnCl_3^-$ and $MnCl_4^-$ geometries have D_{3h} and D_{2d} symmetry, respectively. In $MnCl_5$, 3 Cl atoms are bound dissociatively to the central atom, while 2 Cl atoms

TABLE I. Comparison of our B3LYP results to the RCCSD(T) results[a] and experimental data for MnF and its ions.

		B3LYP/6-311+G(3*df*)			RCCSD(T)/5-ζ basis		
Species	State	r_e (Å)	D_e (eV)	IE (eV)	r_e (Å)	D_e (eV)	IE (eV)
MnF, calc.	$^7\Sigma^+$	1.843	4.65	7.99	1.840	4.68	8.0 ± 0.1
Expt.		1.8387[b]	4.61 ± 0.08[c]				
MnF^+	$^6\Sigma^+$	1.742	4.18		1.750	3.99	
MnF^-	$^6\Sigma^+$	1.902	2.53	1.34	1.908	2.51	1.13

[a]See Ref. 41.
[b]See Ref. 42.
[c]See Ref. 43. A D_o value, the zero point vibrational energy contribution taken from the B3LYP harmonic frequency calculations is −0.04 eV.

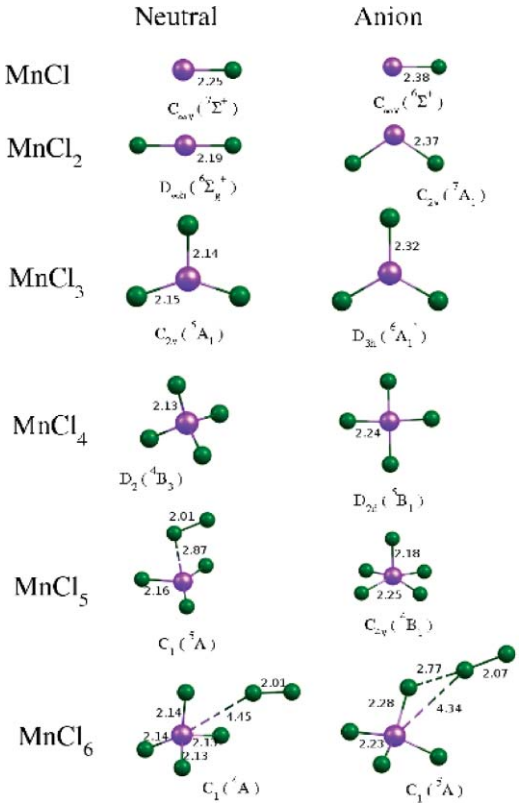

FIG. 1. Optimized geometries of neutral and singly negatively charged $MnCl_n$ clusters. Bond lengths are in (Å).

are attached molecularly, and the geometry corresponds to a $MnCl_3$*Cl_2 adduct. The molecular nature of Cl_2 in this adduct can be confirmed by the bond length of 2.01 Å in the adduct's Cl_2 dimer, which practically matches the equilibrium bond length of 2.00 Å in the free-standing Cl_2 dimer computed at the same level of theory. On the contrary, all Cl atoms are bound to the Mn atom chemically in the $MnCl_5^-$ anion whose ground-state geometry has C_{4v} symmetry. In both $MnCl_6$ and $MnCl_6^-$, four Cl atoms are bound chemically to the Mn atom, while two Cl atoms are bound molecularly, and these species possess the adduct $MnCl_4$*Cl_2 geometries. Our results obtained for the neutral and negatively charged Mn chlorides allow one to state that the highest oxidation state of Mn with respect to Cl is +4.

In neutral $MnCl_n$, the total magnetic moment decreases from 6 μ_B in MnCl to 3 μ_B in $MnCl_4$, i.e., each added Cl atom decreases the total magnetic moment by 1 μ_B in this series. Since $MnCl_5$ can be viewed as a $MnCl_3$*Cl_2 adduct, it has the same total magnetic moment as $MnCl_3$. By analogy, $MnCl_6$ has the same total magnetic moment as $MnCl_4$. Except for $MnCl^-$ and $MnCl_5^-$, the total magnetic moment of an anion is larger by 1 μ_B than the total magnetic moment of the corresponding neutral parent. The total magnetic moment of $MnCl_5^-$ is smaller by 1 μ_B than that of the total magnetic moment of neutral $MnCl_5$ due to the increase in the number of chemically bound Cl atoms: three Cl atoms attached chemically to the Mn atom in $MnCl_5$ vs five atoms attached chemically in $MnCl_5^-$. Both neutral and anionic $MnCl_6$ clusters have adduct-type AX_4*X_2 geometries and, therefore, their total magnetic moments are the same as those of $MnCl_4$ and $MnCl_4^-$, respectively.

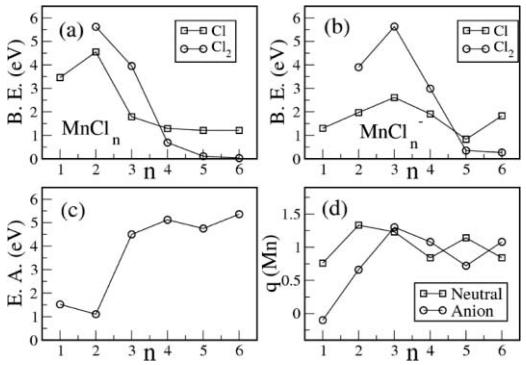

FIG. 2. Calculated energies (BE) of (a) neutral and (b) anionic $MnCl_n$ clusters corresponding to the smallest energy decay channels that yield atomic and molecular Cl. (c) The EA_{ad} of neutral $MnCl_n$. (d) The NAO charge on the Mn atom in neutral and anionic $MnCl_n$ clusters.

Relative thermodynamic stabilities of $MnCl_n$ clusters are estimated from the energies computed for different decay channels. The smallest dissociation energies of the neutral species are to be obtained according to the formula:

$$\Delta E_{neutral} = E(MnCl_n) - E(MnCl_{n-m}) - E(Cl_m), \quad m = 1, 2. \quad (1)$$

while for the anions, one have to estimate the energies of four decay channels according to the formulas:

$$\Delta E^1_{anion} = E(MnCl_n^-) - E(MnCl_{n-m}^-) - E(Cl_m), \quad m = 1, 2. \quad (2a)$$

$$\Delta E^2_{anion} = E(MnCl_n^-) - E(MnCl_{n-m}) - E(Cl_m^-), \quad m = 1, 2. \quad (2b)$$

Figure 2 presents the fragmentation energies of neutral and anionic $MnCl_n$ clusters computed according to these formulas. For n = 1–3, neutral $MnCl_n$ would likely prefer to dissociate into $MnCl_{n-1}$ + Cl, while the lowest energy fragmentation channel for larger n corresponds to the yield of Cl_2. As can be seen from Fig. 2, $MnCl_2$ is the most stable in the neutral series, which is consistent considering the preferred oxidation state of Mn atom to be +2. The lowest energy decay channel of $MnCl_5$ corresponds to dissociation into $MnCl_3$ + Cl_2, as it can be anticipated on the basis of the adduct geometry of $MnCl_5$ in Fig. 1. The fragmentation energy of $MnCl_5$ is only 0.11 eV and it decreases to 0.03 eV for $MnCl_6$, that is, both these neutrals are of the van der Waals type. Since $MnCl_2$ is thermodynamically the most stable species in the neutral series, it is not surprising that $MnCl_3^-$ is the most stable species in the anion series [see Fig. 2(b)] in agreement with experiment.[37] While the yield of molecular chlorine is energetically preferred in the neutral series beginning with $MnCl_4$, it is $MnCl_5^-$ in the anion series.

As it was stated before, the highest oxidation state of Mn relative to Cl atoms is +4. According to our

TABLE II. Theoretical values of EA, VDE, and ground-state magnetic moments of neutral and anionic $MnCl_n$ clusters.

Cluster	Neutral GS μ (μ_B)	Anion GS μ (μ_B)	EA (eV)	VDE (eV)
MnCl	6	5	1.52	1.59
$MnCl_2$	5	6	1.10	2.00
$MnCl_3$	4	5	4.50	5.05
$MnCl_4$	3	4	5.12	5.67
$MnCl_5$	4	3	4.75	5.45
$MnCl_6$	3	4	5.36	5.97

computations of the thermodynamic stability of Mn chlorides, $MnCl_2$ and $MnCl_3^-$ are the most stable species in the neutral and anionic series, respectively. Therefore, one can conclude that the preferred oxidation state of Mn in chlorides is +2. This corresponds to the participation of only two 4*s* electrons in chemical bonding, whereas the half-filled $3d^5$ shell of Mn atom remains intact. The high total magnetic moment of $MnCl_2$ is mostly due to the spins of 3*d*-electrons occupying localized atomic spin-orbitals of Mn.

The calculated VDEs of $MnCl_n^-$ and the EA_{ad} of neutral $MnCl_n$ are presented in Table II. As can be seen, the EA_{ad} and VDE values are quite different for all Mn chlorides (except for MnCl) apparently due to significant distortions of the neutral geometries produced by the extra electron attachment. While the EA_{ad} values of MnCl and $MnCl_2$ are relatively small, $MnCl_3$ has the EA_{ad} of 4.50 eV and is a superhalogen. The EA_{ad} and VDE values of $MnCl_n$ are larger than the EA of a Cl atom for $n \geq 3$, and, hence, all of them are superhalogens.

In order to gain insight into the nature of chemical bonding in the Mn chlorides, one can analyze the electronic distributions reflected in the charges on atoms computed using natural atomic orbitals (NAO). The Mn charge obtained from the NBO[45] analysis is presented in Fig. 2(d) as a function of *n*. The charge is positive in all neutral $MnCl_n$, which indicates the anticipated metal-to-ligand charge transfer. As can be seen, the Mn charge increases at $n = 2$ and then decreases at $n = 3$ and 4. The Mn charges in $MnCl_5$ and $MnCl_6$ are nearly the same as in $MnCl_3$ and $MnCl_4$, respectively, in accord with the adduct type of $MnCl_5$ ($MnCl_3$*Cl_2) and $MnCl_6$ ($MnCl_4$*Cl_2). In the $MnCl_n^-$ anions, the Mn charge increases up to $n = 3$ and then decreases at $n = 4$ and 5. The Mn charge in $MnCl_6^-$ is the same as it is in $MnCl_4^-$ since the $MnCl_6^-$ anion corresponds to a weakly bound $MnCl_4$*Cl_2^- complex. The Mn charges in neutral MnCl and $MnCl_2$ are significantly larger than the Mn charges in the corresponding anions. This means that the extra electron is mostly localized on the Mn atom in these anions. However, the extra electron is delocalized over halide atoms in the $MnCl_n^-$ anions for $n \geq 3$ and the corresponding neutrals are superhalogens.

It is interesting to compare the properties of $MnCl_3$ with the properties of $MgCl_3$ and $ZnCl_3$, where Mg and Zn possess oxidation states of +2. Unlike the lowest total energy structure of $MnCl_3$, where all Cl atoms are bound dissociatively, the lowest total energy structure of $MgCl_3$ contains[9] non-dissociated quasi-molecular Cl_2, as shown in Fig. 3. The computed $MgCl_3$ EA_{ad} of 5.43 eV is to be compared to

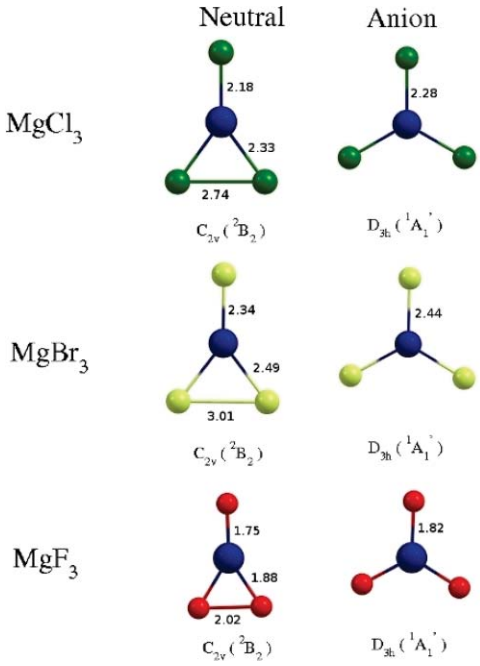

FIG. 3. Ground-state geometries of the neutral and anionic Mg trihalides. Bond lengths are in (Å).

4.50 eV of $MnCl_3$. The computed EA_{ad} of $ZnCl_3$ is 5.40 eV, which practically matches the $MgCl_3$ EA_{ad} value. Both neutral and anionic $ZnCl_3$ geometries are similar to the $MgCl_3$ geometries; therefore, one can assert that both Mg and Zn interact with three chlorine atoms in a similar way. The smaller value of the $MnCl_3$ EA_{ad} compared to the $MgCl_3$ and $ZnCl_3$ EA_{ad} values can be related to the involvement of 3*d* electrons in the Mn–Cl interactions. Indeed, the ground-state total magnetic moment of $MnCl_3$ is 4 μ_B and the total NAO occupation of spin-up 3*d* electrons is 4.58 *e* according to the results of the NBO analysis.

B. $MnBr_n$ clusters

In order to examine how the involvement of the Mn $3d^5$ subshell in the bonding in Mn halides depends on the halide electronegativity, we calculated the properties of Mn bromides and fluorides. First we consider bromides whose optimized geometries are displayed in Fig. 4. The ground-state neutral and anionic geometries of $MnBr_n$ are similar to those of $MnCl_n$ for $n \leq 3$ with the only exception of $MnBr_2^-$, which is linear, while $MnCl_2^-$ is bent. For larger *n*, there are a number of differences between Mn chloride and bromide structures. In neutral $MnBr_4$, only two Br atoms are chemically attached to the Mn atom, while two other Br atoms are attached molecularly. The Br–Br distance in the dimer is 2.37 Å, which is close to the bond length of 2.31 Å in a free-standing Br_2 molecule. All Br atoms are attached chemically to the Mn atom in the $MnBr_4^-$ anion in the same way as in the $MnCl_4^-$ anion. Both neutral $MnBr_5$ and its $MnBr_5^-$ anion contain a Br_2 dimer bound to the $MnBr_3$ core. We have not considered larger $MnBr_n$ clusters because the binding energy of Br_2 already in $MnBr_5$ is very small.

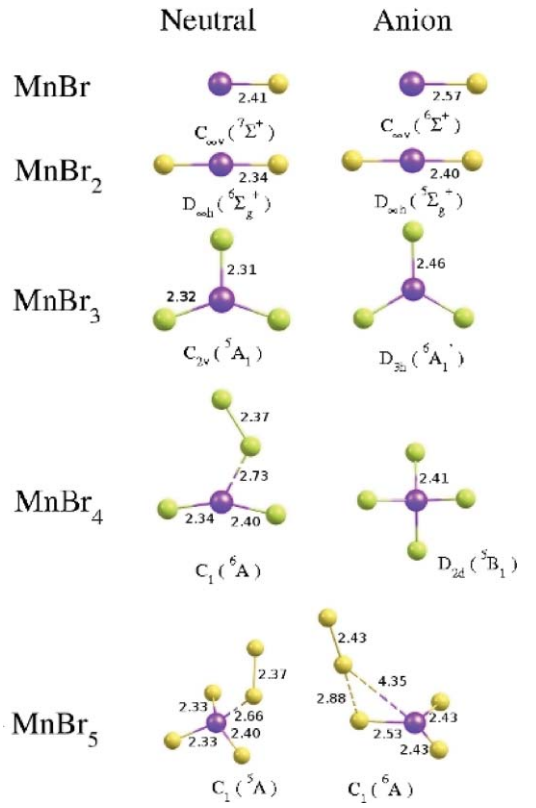

FIG. 4. Optimized geometries of neutral and singly negatively charged $MnBr_n$ clusters. Bond lengths are in (Å).

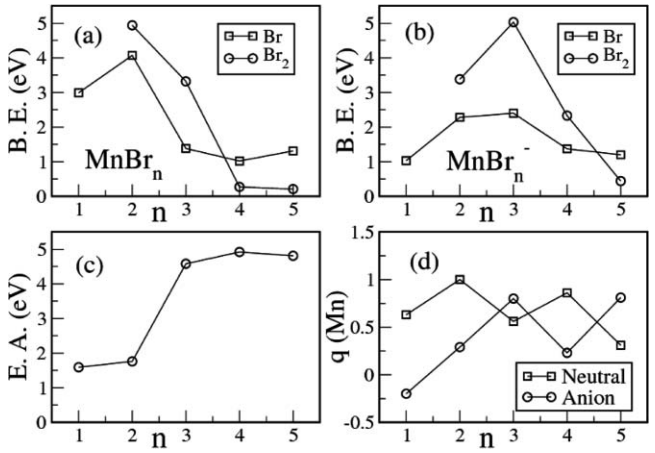

FIG. 5. Calculated energies (BE) of (a) neutral and (b) anionic $MnBr_n$ clusters corresponding to the smallest energy decay channels that yield atomic and molecular Br. (c) The EA_{ad} of neutral $MnBr_n$. (d) The NAO charge on the Mn atom in neutral and anionic $MnBr_n$ clusters.

The total magnetic moments of neutral $MnBr_n$ clusters are 4 μ_B for $n = 3$ and 5 μ_B for $n = 2$ and 4, respectively. $MnBr_4$ has the same magnetic moment as $MnBr_2$ because it has a $MnBr_2$*Br_2 adduct-type geometry. Similarly, the ground-state geometrical structure of $MnBr_5$ can be described as $MnBr_3$*Br_2; therefore, the total magnetic moments of $MnBr_3$ and $MnBr_5$ match each other. The total magnetic moment of $MnBr_2^-$ is 4 μ_B, while it is 6 μ_B in $MnCl_2^-$. The difference is reflected in the different ground-state geometries of $MnBr_2^-$ and $MnCl_2^-$.

The fragmentation energies of neutral and anionic $MnBr_n$ clusters calculated using Eqs. (1) and (2) are displayed in Figs. 5(a) and 5(b), respectively. Similar to the neutral $MnCl_n$ chlorides, the neutral Mn bromides would dissociate to $MnBr_{n-1}$ + Br for $n \leq 3$ and to $MnBr_{n-2}$ + Br_2 for $n = 4$ and 5. The binding energies of $MnBr_4$ and $MnBr_5$ are very small which is consistent with their adduct-type geometries. Among the anionic Mn bromides, the yield of a Br_2 dimer is energetically preferred only for $MnBr_5^-$. The $MnBr_2$ and $MnBr_3^-$ species are the most thermodynamically stable in the neutral and anionic series, respectively. This allows the oxidation state of +2 to be considered as the preferred state in interactions between Mn and Br atoms. This number corresponds to the preferred oxidation state of Mn in chlorides; however, the maximum oxidation state of Mn relative to Br is +3, i.e., one less than relative to Cl.

The calculated VDEs of $MnBr_n^-$ and the EA_{ad} of neutral $MnBr_n$ are presented in Table III. While the EA_{ad} values of MnBr and $MnBr_2$ are smaller than 2 eV, the EA_{ad} of $MnBr_3$ is 4.58 eV, which makes this tribromide a superhalogen. The NAO charge of the Mn atom obtained for the neutral and anionic $MnBr_n$ series is plotted in Fig. 5(d) as a function of n. For the neutral species, the Mn charge oscillates between odd and even n values. In anions, the Mn charge increases up to $n = 3$, decreases at $n = 4$, and increases again at $n = 5$. According to this plot, the extra electron is mostly localized at Mn in $MnBr^-$ and $MnBr_2^-$. This can be related to the relatively low EA_{ad} values of their neutral parents. In $MnBr_3^-$ cluster, the extra electron is delocalized over the ligand atoms, which is typical for superhalogens. There is no substantial increase in the EA_{ad} of $MnBr_4$ and $MnBr_5$ compared to the EA_{ad} of $MnBr_3$. The calculated VDE and EA_{ad} values of $MnCl_3$ and $MnBr_3$ clusters are underestimated with respect to the experimental values by about 0.5 eV, which is in agreement with the previously reported theoretical values.[17] We also calculated the EA_{ad} values of $MnCl_3$ and $MnBr_3$ using the 6–311+(3*df*) basis set and the second-order perturbation theory.[46] The MP2 EA_{ad} values of 5.49 eV and 5.70 eV obtained for $MnCl_3$ and $MnBr_3$, respectively, are overestimated compared to the corresponding experimental values[17] of 5.07 ± 0.06 eV and 5.03 ± 0.06 eV.

The total magnetic moment of the lowest total energy state of $MnBr_3$ is 4 μ_B and the 3*d* shell occupation is 4.70 *e*, which is to be compared to 4.58 *e* in $MnCl_3$. The larger occupation of 3*d* electrons in $MnBr_3$ indicates that Mn–Br interactions are weaker than the Mn–Cl interactions. Appar-

TABLE III. Theoretical values of EA, VDE, and ground-state magnetic moments of neutral and anionic $MnBr_n$ clusters.

Cluster	Neutral GS μ (μ_B)	Anion GS μ (μ_B)	EA (eV)	VDE (eV)
MnBr	6	5	1.59	1.69
$MnBr_2$	5	4	1.76	1.80
$MnBr_3$	4	5	4.58	4.95
$MnBr_4$	5	4	4.92	5.33
$MnBr_5$	4	5	4.81	5.37

ently, it is due to a larger size of Br atoms compared to Cl atoms, which is reflected in longer Mn–Br bond lengths as compared to the Mn–Cl bond lengths.

We also computed the lowest total energy excited states (ES) of $MnCl_3$ and $MnBr_3$, which were found to possess the same total magnetic moment of 6 μ_B. The excited state geometries are similar to the geometries of the corresponding ground states of $MgCl_3$ and $MgBr_3$ shown in Fig. 3. The 3*d* subshell occupation in these isomers increases to 4.96 *e*, which means that the Mn 3*d* electrons are chemically inert in these exited states. The total energy difference between the ground and excited states of $MnCl_3$ is 0.90 eV and the difference reduces to 0.49 eV in $MnBr_3$. The larger 3*d* electron occupation in ground-state $MnBr_3$ and smaller total energy difference in the ground-excited state in $MnBr_3$ compared to those of $MnCl_3$ confirm interactions of Mn 3*d* electrons with Br electrons to be weaker than with Cl electrons.

C. MnF_n clusters

Optimized geometries of the ground-state MnF_n and MnF_n^- series are shown in Fig. 6. As can be seen, fluorine atoms are attached dissociatively up to $n = 5$ and $n = 6$ in the neutral and anion series, respectively. This behavior is different from that found above for the $MnCl_n$ and $MnBr_n$ series. It is rather surprising that a Mn atom can chemically bind three Br atoms, four Cl atoms, and five F atoms (see Figs. 1, 4, and 6) despite these ligand atoms belong to the same group of halogens. The neutral MnF_6 geometry corresponds to a MnF_4*F_2 adduct, while the MnF_6^- geometry is nearly octahedral. Adding one more F atom to the structures of the hexafluorides results in thermodynamically metastable neutral and anionic MnF_7. Total energies of the MnF_7 and MnF_7^- states shown in the bottom of Fig. 6 are higher than the dissociation limits $MnF_5 + F_2$ and $MnF_5^- + F_2$ by 1.34 eV and 0.23 eV, respectively.

In the neutral MnF_n series, the total magnetic moment decreases monotonously from 6 μ_B of MnF to 2 μ_B of MnF_5. The smallest total magnetic moments found in the $MnBr_n$ and $MnCl_n$ series are 4 μ_B and 3 μ_B, respectively. That is, the value of the smallest total magnetic moment decreases when the halogen size decreases. As anticipated, MnF_6 possesses the same total magnetic moment as MnF_4 cluster because the hexafluoride has an adduct-type MnF_4*F_2 geometry. The total magnetic moment of the MnF_n^- anions is larger than that of the corresponding neutral clusters by 1 μ_B for $n = 3$, 4, and 5.

Fragmentation energies of MnF_n clusters are displayed in Fig. 7. The smallest energy dissociation channel of neutral MnF_n corresponds to $MnF_{n-1} + F$ for $n \leq 5$, and the smallest energy decay channel of anionic MnF_n corresponds to $MnF_{n-1}^- + F$ up to $n = 6$. The MnF_7^- anion shown in Fig. 6 is metastable with respect to the $MnF_5^- + F_2$ decay. Figure 7 shows MnF_2 to be the most thermodynamically stable in the neutral series. However, the thermodynamically most stable anion cluster in the MnF_n^- series is MnF_4^- but not MnF_3^- as would follow from the analogy with the chlorine and bromine series. Judged by the ability of Mn to bind chemically up to 5 fluorine atoms in the neutral MnF_n series, one could assign the maximum oxidation state of +5 to Mn relative to F. However, the maximum oxidation state of Mn relative to F was previously assigned as +4.[28] This discrepancy can be ascribed to a lower thermodynamic stability of MnF_5 with respect to that of MnF_4 [see Fig. 3(c)].

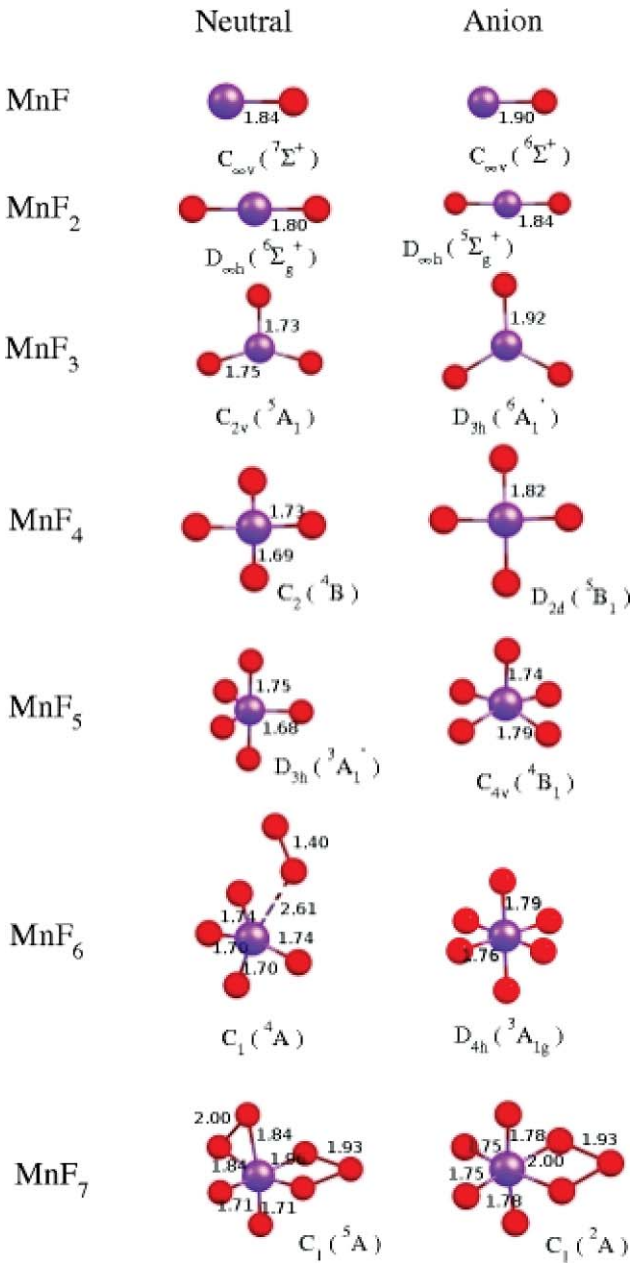

FIG. 6. Optimized geometries of neutral and singly negatively charged MnF_n clusters. Bond lengths are in (Å).

Our calculated VDE and EA_{ad} values of Mn fluorides are given in Table IV. As in the chlorine and bromine series, the EA_{ad} values are relatively small in the beginning of the series and jump up to 3.42 eV at MF_3, which is smaller than the EA of a Cl atom. Note that the EA_{ad} values of both $MnCl_3$ and $MnBr_3$ are higher than the MF_3 EA_{ad} by about 1 eV. The EA_{ad} of the next member in the series, MnF_4, is 5.07 eV and this tetrafluoride is a superhalogen. As in the preceding

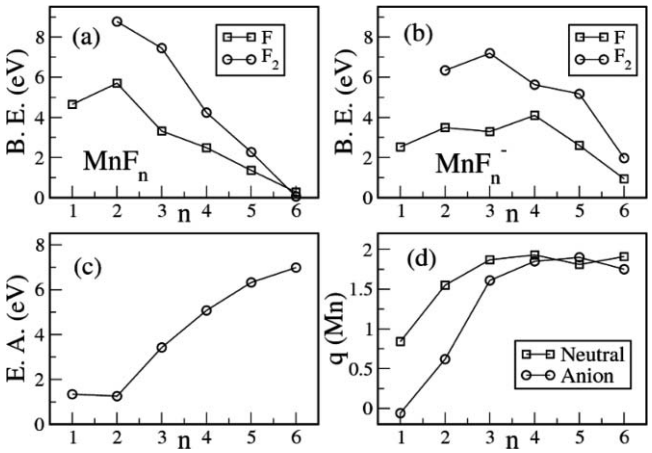

FIG. 7. Calculated energies (BE) of (a) neutral and (b) anionic MnF_n clusters corresponding to the smallest energy decay channels that yield atomic and molecular F. (c) The EA_{ad} of neutral MnF_n. (d) The NAO charge on the Mn atom in neutral and anionic MnF_n clusters.

chloride and bromide series, the VDE and EA_{ad} values are rather different for $n = 3$–7 because an extra electron attachment results in large geometry changes.

The Mn NAO charge in the neutral and anionic MnF_n series is plotted in Fig. 7(d) as a function of n. In the neutral series, the Mn charge increases up to $n = 3$ and then saturates. In the anion series, the Mn charge saturation occurs after $n = 4$. The extra electron is entirely delocalized over fluorine atoms in the MnF_4^- anion, and MnF_4 is a superhalogen. This is not so in the MnF_3^- anion, where the extra electron is partially localized on the Mn atom, and, as a consequence, MnF_3 is not a true superhalogen. This could be due to a rather large involvement of Mn 3*d* electrons in the chemical bonding, which is reflected in the Mn 3*d* population of 4.35 *e*. This is appreciably smaller than the 3*d* subshell occupation in the Mn tribromides and trichlorides. When moving from MnF_4 to MnF_5 and MnF_6, a substantial increase in EA_{ad} values is observed, and the Mn hexafluoride possesses the highest EA_{ad} value in the considered Mn halide series, which exceeds the EA of a Cl atom nearly two times.

The interaction between Mn and F in MnF_3 is different from that between Mn and Cl (Br) in $MnCl_3$ ($MnBr_3$). This is reflected from the following results: (1) The occupancies of 3*d* electrons in the majority spin channel of Mn in MnF_3 are 4.35 *e* while that in $MnCl_3$ and $MnBr_3$ are 4.58 *e* and 4.70 *e*,

TABLE IV. Theoretical values of EA, VDE, and ground-state magnetic moments of neutral and anionic MnF_n clusters.

Cluster	Neutral GS μ (μ_B)	Anion GS μ (μ_B)	EA (eV)	VDE (eV)
MnF	6	5	1.34	1.37
MnF_2	5	4	1.25	1.29
MnF_3	4	5	3.42	4.55
MnF_4	3	4	5.07	6.23
MnF_5	2	3	6.32	7.13
MnF_6	3	2	6.98	7.78

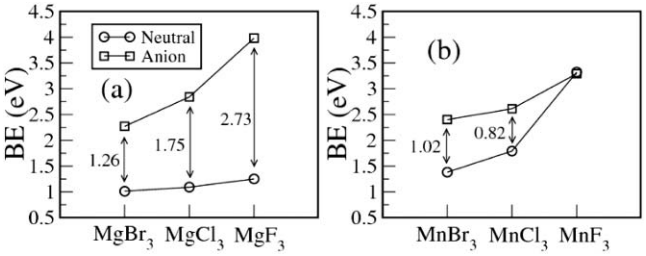

FIG. 8. The differences in the binding energies of the anionic and neutral trihalides: (a) MgX_3; (b) MnX_3.

respectively. (2) The excited state of MnF_3 lies 1.50 eV above the GS, while it is 0.90 eV for $MnCl_3$ and 0.49 eV for $MnBr_3$. (3) The magnetic moment of the ES of MnF_3 is 2 μ_B, while that for $MnCl_3$ and $MnBr_3$ is 6 μ_B. The energy of the 6 μ_B state in MnF_3 is 2.53 eV higher than the GS. Note that the 6 μ_B magnetic moment arises when $3d^5$ electrons behave as inert core. Clearly, this is not the case with the ES of MnF_3.

Finally, we compare the trends in binding energies of MgX_3 and MnX_3 (X = F, Cl, Br). Figure 8 presents the differences in binding energies of the neutrals and its anions computed according to Eqs. (1) and (2). As can be seen, there are opposite trends in the Mg and Mn trihalide series. If the difference in the binding energies of a halogen atom in a neutral MgX_3 cluster and its anion increases when moving from Br to F, then the reverse trend is observed for the Mn trihalides. These trends illustrate the role the Mn 3*d*-subshell plays during interactions with halogen atoms.

IV. CONCLUSIONS

Using density functional theory, we performed a systematic study of interactions of halogen atoms with a single Mn atom. In order to gain insight into the role played by the Mn half-filled 3*d*-shell, we compared the properties of MnX_3 and MgX_3 trihalides. Our results can be summarized as follows:

(i) The interaction of Mn 3*d* electrons with halogen atoms is seen to differ from one halogen atom to another. While the geometries of neutral $MnCl_n$ and $MnBr_n$ bear some resemblance with each other, those of the MnF_n clusters are different. This demonstrates that the $3d^5$ subshell of Mn interacts more strongly with F than with Cl or Br. This is due to the larger electronegativity and smaller size of fluorine atoms that permit them come closer to the Mn atom.

(ii) By analogy to the classic $MgCl_3$ *sp*-superhalogen, $MnCl_3$ and $MnBr_3$ are superhalogens as well, but not MnF_3 whose adiabatic electron affinity nearly matches the EA of the F atom. This allows one to assign the preferred oxidation number of +2 for Mn interacting with Cl or Br, and +3 relative to F.

(iii) The adiabatic electron affinity of $MgBr_3$ is larger than that of $MgCl_3$, which, in turn, is larger than that of MgF_3. The difference between the calculated electron affinities of $MnCl_3$ and $MnBr_3$ clusters is only 0.08 eV,

which is in good agreement with the experimental value of 0.04 eV.

(iv) In the anion series, $MnCl_3^-$, $MnBr_3^-$, and MnF_4^- are thermodynamically the most stable species.

ACKNOWLEDGMENTS

This work was partially supported by a grant from the Defense Threat Reduction Agency (Grant No. HDTRA1-09-1-0025). This research used resources of the National Energy Research Scientific Computing Center, which is supported by the Office of Science of the U.S. Department of Energy (Contract No. DE-AC02-05CH11231).

[1]N. Bartlett, Proc. Chem. Soc., London **6**, 218 (1962).
[2]N. Bartlett and D. H. Lohmann, Proc. Chem. Soc., London **3**, 115 (1962).
[3]G. L. Gutsev and A. I. Boldyrev, Chem. Phys. **56**, 277 (1981).
[4]G. L. Gutsev and A. I. Boldyrev, Chem. Phys. Lett. **108**, 250 (1984).
[5]M. K. Scheller, R. N. Compton, and L. S. Cederbaum, Science **270**, 1160 (1995).
[6]G. L. Gutsev and A. I. Boldyrev, Zh. Neorg. Khim. (Russ.) **26**, 2353 (1981).
[7]H. Hotop and W. C. Lineberger, J. Phys. Chem. Ref. Data **14**, 731 (1985).
[8]X.-B. Wang, C.-F. Ding, L.-S. Wang, A. I. Boldyrev, and J. Simons, J. Chem. Phys. **110**, 4763 (1999).
[9]B. M. Elliot, E. Koyle, A. I. Boldyrev, X.-B. Wang, and L.-S. Wang, J. Phys. Chem. A **109**, 11560 (2005).
[10]I. Anusiewicz and P. Skurski, Chem. Phys. Lett. **358**, 426 (2002).
[11]I. Anusiewicz, M. Sobczyk, I. Dabkowska, and P. Skurski, Chem. Phys. **291**, 171 (2003).
[12]C. Sikorska, S. Smuczynska, P. Skurski, and I. Anusiewicz, Inorg. Chem. **47**, 7348 (2008).
[13]G. L. Gutsev, P. Jena, and R. J. Bartlett, Chem. Phys. Lett. **292**, 289 (1998).
[14]G. L. Gutsev and A. I. Boldyrev, Mol. Phys. **53**, 23 (1984).
[15]G. L. Gutsev and A. I. Boldyrev, Chem. Phys. Lett. **101**, 441 (1983).
[16]K. Pradhan, G. L. Gutsev, and P. Jena, J. Chem. Phys. **133**, 144301 (2010).
[17]X. Yang, X.-B. Wang, L.-S. Wang, S. Q. Niu, and T. Ichiye, J. Chem. Phys. **119**, 8311 (2003).
[18]J. Yang, X.-B. Wang, X.-P. Xing, and L.-S. Wang, J. Chem. Phys. **128**, 201102 (2008).
[19]G. L. Gutsev, P. Jena, H.-J. Zhai, and L.-S. Wang, J. Chem. Phys. **115**, 7935 (2001).
[20]G. L. Gutsev, C. A. Weatherford, K. Pradhan, and P. Jena, J. Phys. Chem. A **114**, 9014 (2010).
[21]K. Pradhan, G. L. Gutsev, C. A. Weatherford, and P. Jena, J. Chem. Phys. **134**, 144305 (2011).
[22]S. Smuczynska and P. Skurski, Chem. Phys. Lett. **443**, 190 (2007).
[23]D. F. Hunt, G. C. StaffordJr., F. W. Crow, and J. W. Russell, Anal. Chem. **48**, 2098 (1976).
[24]F. Arnold, Nature (London) **284**, 610 (1980).
[25]J. C. Champarnaud-Mesjard and B. Frit, Solid State Sciences **29**, 161 (1992).
[26]N. Bartlett, G. Lucier, and C. Shen, J. Fluorine Chem. **71**, 163 (1995).
[27]G. L. Gutsev, B. K. Rao, P. Jena, X.-B. Wang, and L. S. Wang, Chem. Phys. Lett. **312**, 598 (1999).
[28]S. Riedel and M. Kaupp, Coord. Chem. Rev. **253**, 606 (2009).
[29]A. D. Becke, J. Chem. Phys. **98**, 5648 (1993).
[30]J. M. Wittbrodt and H. B. Schlegel, J. Chem. Phys. **105**, 6574 (1996).
[31]R. Krishnan, J. S. Binkley, R. Seeger, and J. A. Pople, J. Chem. Phys. **72**, 650 (1980).
[32]A. D. Mclean and G. S. Chandler, J. Chem. Phys. **72**, 5639 (1980).
[33]K. Yang, J. Zheng, Y. Zhao, and D. G. Truhlar, J. Chem. Phys. **132**, 164117 (2010).
[34]F. Neese, Coord. Chem. Rev. **253**, 526 (2009).
[35]S. F. Sousa, P. A. Fernandes, and M. J. Ramos, J. Phys. Chem. A **111**, 10439 (2007).
[36]K. E. Riley, B. T. Op't Holt, and K. M. Merz, Jr., J. Chem. Theory Comput. **3**, 407 (2007).
[37]M. M. Wu, H. Wang, Y. J. Ko, Q. Wang, Q. Sun, B. Kiran, A. K. Kandalam, K. H. Bowen, and P. Jena, Angew. Chem., Int. Ed. **50**, 2568 (2011).
[38]R. J. Bartlett and M. Musial, Rev. Mod. Phys. **79**, 291 (2007).
[39]R. Cracium, R. T. Long, D. A. Dixon, and K. O. Christe, J. Phys. Chem. A **114**, 7571 (2010).
[40]R. Cracium, D. Picone, R. T. Long, S. Li, D. A. Dixon, K. A. Peterson, and K. O. Christe, Inorg. Chem. **49**, 1056 (2010).
[41]S. Kardahakis, C. Koukounas, and A. Mavridis, J. Chem. Phys. **122**, 054312 (2005).
[42]O. Launila, B. Simard, and A. M. James, J. Mol. Spectrosc. **159**, 161 (1993).
[43]G. Balducci, M. Campodonico, G. Gigli, G. Meloni, and S. N. Cesaro, J. Chem. Phys. **117**, 10613 (2002).
[44]M. J. Frisch, G. W. Trucks, H. B. Schlegel *et al.*, GAUSSIAN 03, Revision C.02, Gaussian, Inc., Wallingford, CT, 2004.
[45]A. E. Reed, L. A. Curtiss, and F. Weinhold, Chem. Rev. **88**, 899 (1988).
[46]M. Head-Gordon, J. A. Pople, and M. J. Frisch, Chem. Phys. Lett. **153**, 503 (1988).